

Barrier to complete fusion for ${}^4\text{He}$ and ${}^1\text{H}$ and that for evaporation from ${}^{194}\text{Hg}$

M. A. McMahan

Department of Chemistry, Columbia University, New York, New York 10027

John M. Alexander

Department of Chemistry, State University of New York at Stony Brook, Stony Brook, New York 11794

(Received 21 March 1979)

A reference set of transmission coefficients for ${}^1\text{H}$ and ${}^4\text{He}$ reactions is obtained by systematic fits to data for fusion cross sections. Comparisons to other sets, obtained from elastic scattering data, show some significant differences. A comparison is made of calculated to measured evaporation spectra for ${}^4\text{He}$ from ${}^{194}\text{Hg}$ ($E^* = 98$ MeV, $l_{\text{crit}} = 45$). There appears to be a significant reduction in the barrier to evaporation for this excited nucleus.

[NUCLEAR REACTIONS Fusion cross sections for ${}^1\text{H}$ - and ${}^4\text{He}$ -induced reactions are systematized to provide reference values for transmission coefficients. Evaporation spectrum analysis made for ${}^4\text{He}$ from ${}^{194}\text{Hg}$ ($E^* = 98$ MeV, $l_{\text{crit}} = 45$).]

I. INTRODUCTION

Through the years a reasonable body of quantitative experimental data has appeared on capture¹⁻⁸ and evaporation reactions⁹⁻¹⁴ for ${}^1\text{H}$ and ${}^4\text{He}$. The close relationship of emission processes to capture processes is embodied in the principle of detailed balance on which nuclear evaporation theory rests.¹⁵⁻¹⁷ The rate of evaporation is expressed in terms of level densities of emitting and residual nuclei and the inverse reaction (or partial wave) cross section. As these inverse (or capture) cross sections cannot be measured for target nuclei in excited states one usually begins an evaporation analysis with estimates obtained from interactions between ground-state nuclei.¹⁵⁻¹⁷ The sources of data for these estimates are of two types: (a) elastic scattering and (b) reaction cross sections. From such data one obtains parameters for an optical potential which are systematized in some way for general application.

By its very nature an important part of nuclear evaporation processes favors emission energies near and even below the Coulomb barrier.¹⁵⁻¹⁷ In this energy region the capture cross sections and transmission coefficients are rapidly varying functions of energy and l . Therefore, the calibration of parameters of the model potential is quite important.¹⁰ The purpose of this paper is to reexamine the logical and data bases for these calibrations. Most commonly one has used optical-model parameters obtained from comparisons to elastic scattering data. In recent years it has been generally accepted that the elastic scattering is only sensitive to the real potential at distances well beyond the s -wave barrier distance.^{3,18,19} On the

contrary, fusion cross sections at low energy are especially sensitive to the height of the s -wave barrier and its penetrability.^{3,20-22} We propose that calibrations of transmission coefficients for capture processes should emphasize their direct relationship to fusion cross sections. We have searched the literature for relevant cross section data and we propose simple parametrizations that can be easily generalized.

II. LOGIC AND TECHNIQUES

A. General background

In recent studies, Vaz *et al.* have examined the relationship between the optical model and cross sections for elastic scattering, complete fusion, and all reactive collisions.²⁰⁻²² For the system ${}^{16}\text{O} + {}^{208}\text{Pb}$ there is an abundance of high-quality data for each of these processes.^{23,24} Even though data of comparable extent are not available for H or He induced reactions, we can probably expect that many aspects are similar. What are the general features that concern us most? (i) Optical-model parametrizations that account for elastic scattering at high energies usually do not work well at low energies for either complete fusion or elastic scattering.^{3,18-20} (ii) Very good fits to elastic scattering require an energy dependent parametrization^{18-20,24} that requires a large data base to establish. (iii) A more simple energy independent potential parametrization can account for cross sections for fusion, all reactions, and for the quarter-point angles in elastic scattering.²⁰⁻²² The systematics of these energy independent parameters are much more easily established than those based on elastic scattering alone.

These observations have caused us to rethink the logic and parametrization procedure for optical potentials to be used in evaporation calculations. Consider the equilibrium evaporation of a spinless particle ν from an emitting nucleus A to final nucleus B ¹⁵⁻¹⁷:

$$A(E_A, J_A \dots) \rightarrow B(E_B, J_B \dots) + \nu(\epsilon_\nu, l). \quad (1)$$

Energy and angular momentum conservation are given by

$$E_A = E_B + S_\nu + \epsilon_\nu, \quad (2)$$

and

$$\vec{J}_A = \vec{J}_B + \vec{l}. \quad (3)$$

Excitation energies of A and B are denoted by E , spins by J ; kinetic energy, separation energy, and orbital angular momentum of the ν , B exit channel are labeled by ϵ_ν , S_ν , and $l\hbar$. The inverse partial wave cross sections for B (excited to E_B, J_B) in Eq. (1) are given by

$$\sigma_l(\epsilon_\nu) = (2l+1)\pi\chi^2 T_l(\epsilon_\nu)_{B+\nu}, \quad (4)$$

with their sum over l the cross section for formation of the A nucleus (excited to E_A, J_A) at equilibrium¹⁵⁻¹⁷

$$\sigma(\epsilon_\nu) = \sum \sigma_l(\epsilon_\nu) = \sum_{l=0}^{\infty} (2l+1)\pi\chi^2 T_l(\epsilon_\nu). \quad (5)$$

As we cannot, in general, measure cross sections involving excited nuclei, we must try to systematize those for ground-state nuclei which must then be considered only as reference values. If these reference values of $T_l(\epsilon_\nu)$ lead to a good description of measured evaporation spectra, then we can conclude that the effective potentials for the excited nuclei are undistinguishable for the exit channels $B(E_B, J_B \dots) + \nu(l)$ and for our reference set. As excitation energy E_B and spin J_B are increased one does expect nuclear deformations²⁵ or expansions^{26,27} to occur to some extent, and the detailed form of the evaporation spectra may provide an understanding of these effects.^{9,13,17}

What is the most appropriate way to develop a parametrization to describe the needed reference set of transmission coefficients? Most commonly in the past an optical potential parametrization has been obtained from elastic scattering data, often obtained at energies well above the barrier. Parameters obtained at high energy have been shown to be unsatisfactory at near-barrier energies.^{18,24} Barnett and Lilley have made a careful study of both scattering and reaction (or fusion) cross sections at near-barrier energies.³ They show that potential parametrizations from scattering data alone give a poor description of the

reaction data at low energies. This is partly due to the different inherent sensitivities of reaction and scattering cross sections¹⁹ (at fixed energy). It could also be due to the presence of inelastic or other soft reactive collisions that blur the boundary between scattering and the fusing collisions that we seek. Scattering data are of great value in setting constraints on the complete optical potential, but in general their power is focused on distances beyond that where the fusion decision is made.^{3,18-21} Therefore, the measured cross sections for complete fusion seem to us to be the best source of data for construction of a reference set of T_l values.¹⁵⁻¹⁷

There is, however, some ambiguity concerning the definition of complete fusion. Typically for heavy ion induced reactions one approximates the fusion cross section as that for fission plus that for forward-peaked residual nuclei.²⁸ For H and He induced reactions the evaporation residues have so far only been measured via radiations from the product nuclei. Products are then selected as predominantly from the compound nucleus mechanisms. Fission is important for near-barrier energies only for actinide targets,²⁹ and for U and Np this is the dominant decay mode for the fused compound nuclei.^{5,6,8}

The major features of the excitation functions for fusion are the rapid rise with energy near the barrier followed by a tendency to level off at higher energies. For near-barrier energies, data have been reported for fusion of ${}^4\text{He}$ with Co,¹ Dy,² Pb,³ Bi,^{3,4} U,⁵ and Np,⁶ and for ${}^1\text{H}$ with Cd,⁷ La,⁷ and U.⁸ For energies comfortably above the barrier a number of "total reaction cross sections" have been reported.³⁰ For intermediate and heavy nuclei ($A > 27$) these measurements can be taken as a close upper limit to the complete fusion cross section,^{2,20,21} and thus can set limits on the fusion radii.

B. Equations and parameters

Vaz *et al.* have discussed the relationships between reaction and fusion cross sections and the optical potential.²⁰⁻²² They have also tested the applicability of certain simple approximate calculations. For H and He induced reactions the range of l values is rather small, and the Wong formulation³¹ can be taken as a good approximation. The cross section ($\sigma \equiv \sigma_{cf}$ for this study) is given in terms of three parameters, E_0 , $\hbar\omega_0$, and R_0 ,

$$\sigma(E) = (R_0^2/2)(\hbar\omega_0/E) \ln \{1 + \exp [2\pi(E - E_0)/\hbar\omega_0]\}. \quad (6)$$

These parameters are related to an inverted parabolic barrier for s waves as shown in Fig. 1. Var-

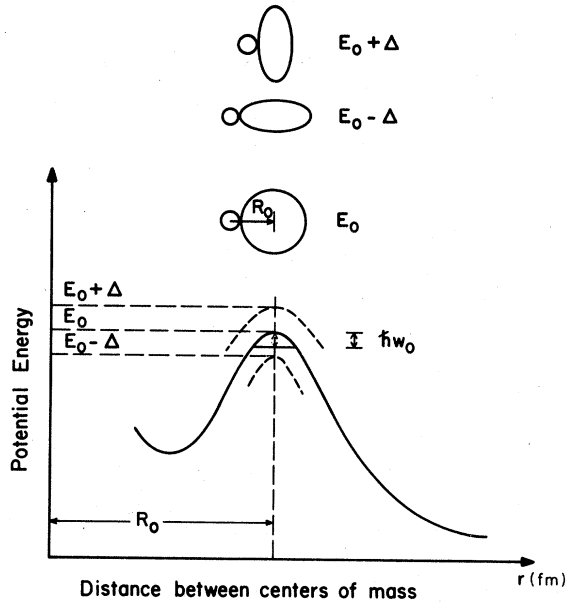


FIG. 1. Schematic diagram of the parametrization used for Hill-Wheeler transmission coefficients.

ious orientations with respect to a deformed²⁵ or vibrating³² nucleus can be allowed for by consideration of a spectrum of barrier heights from $E_0 - \Delta$ to $E_0 + \Delta$. Equation (6) is derived by integrating Eq. (5) with Hill-Wheeler transmission coefficients³³:

$$T_l(E) = \{1 + \exp[2\pi(E_l - E)/\hbar\omega_l]\}^{-1}, \quad (7)$$

and the approximation that

$$E_l = V_N(R_l) + V_0(R_l) + \hbar^2 l(l+1)/2\mu R_l^2, \quad (8)$$

with

$$R_l = R_0 \quad (9)$$

and

$$\hbar\omega_l = \hbar\omega_0. \quad (10)$$

It is convenient for systemization to define the parameters r_0 and r_e

$$R_0 = r_0 A^{1/3} + R_2 \quad (11)$$

and

$$E_0 = Z_1 Z_2 e^2 / R_e = Z_1 Z_2 e^2 / (r_e A^{1/3} + R_2), \quad (12)$$

where R_2 (in fm) is 1.44 for ${}^1\text{H}$ and 2.53 for ${}^4\text{He}$.³⁰ An empirical set of values of R_0 has been obtained for total reaction cross sections at energies well over the barrier where uncertainties in E_0 values have little effect. These empirical values are tabulated in Ref. 30 for 21 reactions induced by ${}^4\text{He}$ and 36 reactions induced by ${}^1\text{H}$. An average value of 1.42 fm was found for r_0 . In Refs. 20 and 22 we

show this value of r_0 for ${}^{16}\text{O} + {}^{208}\text{Pb}$ gives a slight underestimate of the s -wave fusion radius. Systematics of fusion barriers for heavy ion reactions with $Z_1 Z_2 < 500$ also indicate somewhat larger values of r_0 as given by the relationship²²

$$r_0 = 2.0337 - 0.2412 \log_{10}(Z_1 Z_2). \quad (13)$$

These results were based on empirical modification of the proximity potential for gently curved surfaces.³⁴ As the α particle is so small, it may not be appropriate to term its surface as gently curved. Nevertheless, we use Eq. (13) as an upper limit to r_0 and 1.42 fm as a lower limit. [Actually the difference is not very important because r_0^2 enters Eq. (6) simply as a multiplier and not in the exponent.] If we assume that the barrier distances R_0 are rather well constrained,^{22,30} then the main task for us here is to systematize empirical values of fusion barrier heights and their penetrabilities.

For near-barrier energies the other three parameters (r_e , $\hbar\omega_0$, and Δ) control the position and slope of the curves as shown in Fig. 2. The roles of Δ and $\hbar\omega_0$ are not easily distinguished and, in fact, have been shown to change only slightly from spherical to rather highly deformed targets.³⁵ Therefore, for this survey we set $\Delta \equiv 0$ and obtain fits with two free parameters, $\hbar\omega_0$ and r_e (or E_0). We find that the empirical values of $\hbar\omega_0$ are not very different; hence, we take an average value of $\hbar\omega_0 = 3.8$ MeV and fit the data again with only one free parameter r_e . (The failure to observe large increases in empirical values of $\hbar\omega_0$ for statically deformed nuclei³⁵ may indicate that deformation enhances mainly the soft reactive collisions rather than the fusing collisions.) Clearly a parabola cannot realistically represent the shape of the nuclear plus Coulomb potentials for $E \ll E_0$. However, to

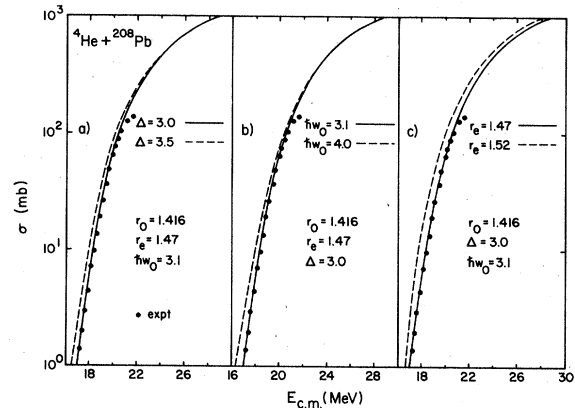


FIG. 2. Effect of the parameters Δ , $\hbar\omega_0$, and r_e (or E_0) on the shape of $\sigma(E)$.

the extent that Eq. (6) can provide a good empirical fit to $\sigma(E)$ for low energies, we can infer that Eq. (7) will provide good empirical values of the transmission coefficients. Thus the values of $\hbar\omega_0$ should be viewed as empirical tools rather than parameters that actually describe the barrier curvatures. This point is discussed further in the appendix.

III. RESULTS

Fits to the steep parts of several excitation functions are shown in Figs. 3–5. In each case measurements were made for a limited number of reaction products (see Table I) so the data should lag below the total fusion cross section as energy increases. As the values of R_0 have been fixed separately^{22,30} the effect of this incompleteness is not serious. Calculations are also shown for the “global” optical-model parametrization of Refs. 36 and 37. (Saxon-Woods parameters: for ${}^4\text{He}$ $V=50.2$ MeV, $r_w=r_v=1.2+1.5A^{-1/3}$, $a_v=a_w=0.564$ fm, $W=12.3$ MeV, $r_c=1.3$ fm; for ${}^1\text{H}$ $V=53.3-0.55E+27(N-Z)/A-0.42/A^{2/3}$, $r_w=r_v=1.25$ fm, $a_v=0.65$ fm, $W=13.5$ MeV, $a_w=0.47$ fm.) These optical-model parameters give cross sections that are close to the data for Co, but are less steep than the data for Dy and Pb. These differences are quite significant for the calculation of evaporation spectra. (See Figs. 7 and 8 later.)

The fits in Figs. 3–5 are adequate even when ob-

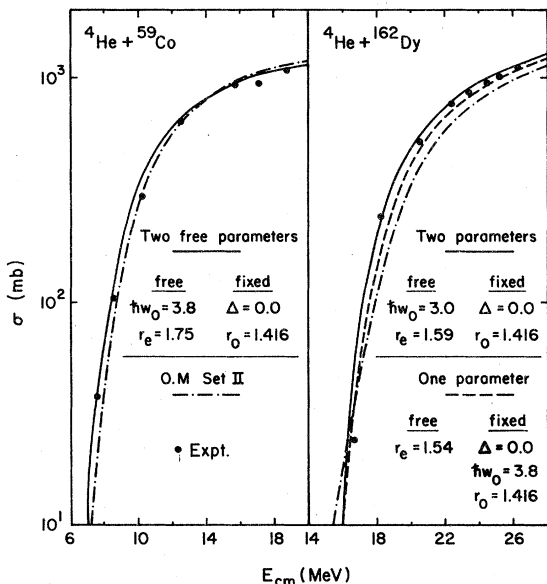


FIG. 3. Fits of Eq. (6) to data for the reactions indicated with one free parameter — — — and two free parameters ——. For comparison, calculations are shown for one optical-model parametrization labeled OM II (Ref. 36).

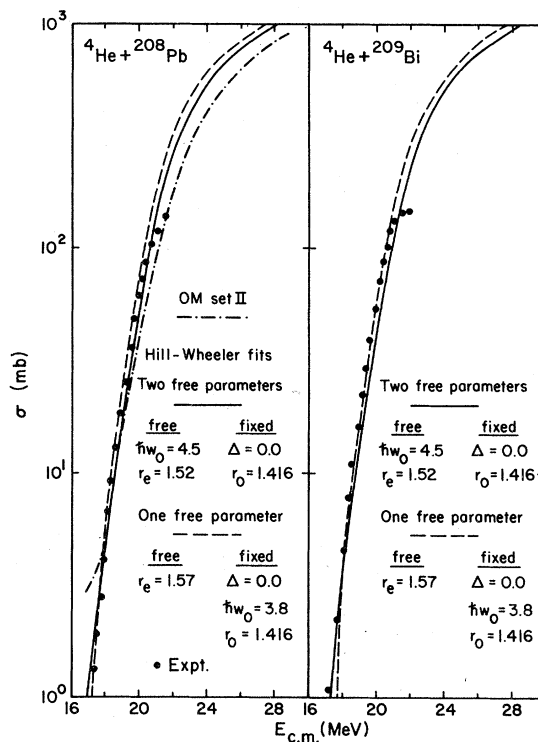


FIG. 4. Same as for Fig. 3.

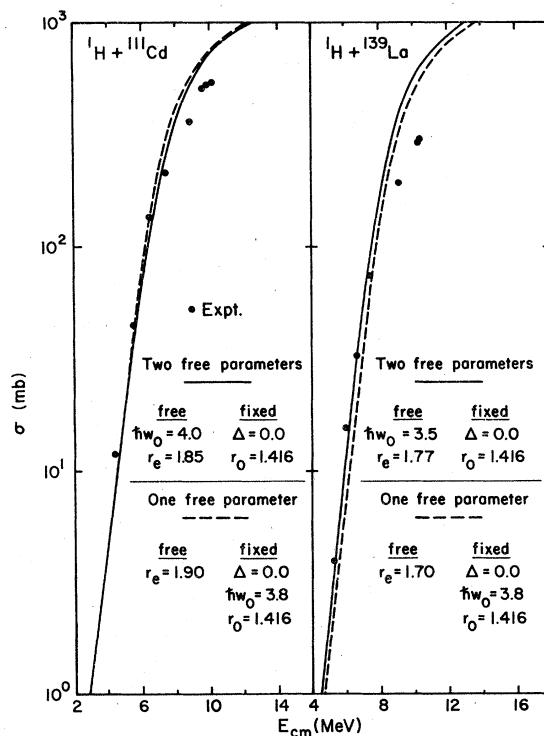


FIG. 5. Same as for Fig. 3.

TABLE I. Fusion cross sections and fitting parameters.

Target	Energy span (MeV in laboratory)	Reactions included	Fitting parameters ^a			Ref.
			one free ^b r_e (fm)	two free ^c r_e (fm)	$\hbar\omega_0$ (MeV)	
${}^{59}\text{Co}$	8.0–18.7	$({}^4\text{He}, n + p + \alpha)$	1.75	1.75	3.8	1
${}^{162}\text{Dy}$	17.5–27	$({}^4\text{He}, n + 2n + 3n)$	1.54	1.59	3.0	2
${}^{208}\text{Pb}$ ^a	16–21	$({}^4\text{He}, n)$	1.57	1.52	4.5	3, 4
${}^{209}\text{Bi}$ ^a	16–21	$({}^4\text{He}, n + 2n + 3n)$				
${}^{233}, {}^{238}\text{U}$ ^a	15–25	$({}^4\text{He}, f + n + 2n)$	1.55	1.51	4.5	5, 6
${}^{237}\text{Np}$ ^a	17.5–22	$({}^4\text{He}, f + n + 2n)$				
${}^{111}\text{Cd}$ ^a	2.1–10.1	$({}^1\text{H}, n)$	1.90	1.85	4.0	7
${}^{139}\text{La}$ ^a	4.5–10.3	$({}^1\text{H}, n)$	1.70	1.77	3.5	7
${}^{233-6}, {}^{238}\text{U}$ ^a	4.5–13.5	$({}^1\text{H}, f + xn)$	1.82	1.82	3.8	8

^aThese one and two parameter fits systematically overestimate the measured cross sections of less than 1 mb. For ${}^{194}\text{Hg}$ this inadequacy is for energies below the range of interest for evaporation calculations (see Figs. 8 and 9 and the Appendix).

^bFixed parameters were $\hbar\omega_0 = 3.8$ MeV, $\Delta = 0$, and $r_0 = 1.42$ fm or from Eq. (13) with no appreciable difference.

^cFixed parameters were $\Delta = 0$ and r_0 as in (b) above.

tained with only r_e as a free parameter ($\hbar\omega_0$ set to its average value and r_0 taken from Refs. 22 or 30). Therefore, the effective barriers contained in the value of r_e can be said to be the most important determinant of the reference parameter set. The empirical values of r_e are given in Table I for one and two parameter fits. These values are somewhat different from those in Ref. 30 because we have set $\Delta \equiv 0$. The values of r_e for the one parameter fits can be represented by the following equations

$$r_e = 2.452 - 0.408 \log_{10} Z_1 Z_2 \text{ fm for } {}^4\text{He}, \quad (14)$$

$$r_e = 1.81 \text{ fm for } {}^1\text{H}. \quad (15)$$

For ${}^4\text{He}$ incident on targets between Co and Bi the small deviations from Eq. (14) imply that the effective barriers can be estimated to $\pm 2\%$. For ${}^1\text{H}$ the data base is weaker, but perhaps $\approx \pm 5\%$ is a reasonable estimate of uncertainties in r_e values for ${}^1\text{H}$ from Eq. (15).

In Figs. 6 and 7 we show transmission coefficients obtained from these fits to fusion cross sections compared to those from some of the global optical-model parametrizations. Several general observations can be made concerning the differences between the HW curves [Hill-Wheeler formula, Eq. (7)] and those from OM I (Ref. 38) and II (Refs. 36 and 37): (i) Invariably, the HW transmission coefficients attain a value of 0.99 at lower energy than do those from OM I or II. Transparency is inferred from optical-model fits to scattering at high energies. Transparency is not an explicit part of Eq. (6); nevertheless, its effects on experimental data will clearly enter into the parametrization, in particular at higher energies

in the values of R_0 . (ii) Invariably for higher l values the slopes of the HW curves are steeper than those for OM II. Presumably this is due to the different radial dependencies for absorption. The HW equation only gives absorption inside R_0 , and there the absorption is complete. However, a Saxon-Woods imaginary potential will give small but significant absorptions at larger distances and some transmission through the nuclear interior. The extent of this transmission at near-barrier energies is very difficult to test experimentally. Ericson

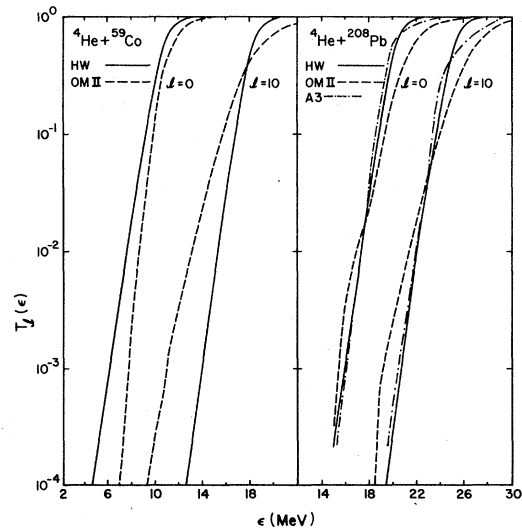


FIG. 6. Transmission coefficients $T_l(\epsilon)$ vs channel energy ϵ for the indicated reactions. Hill-Wheeler parameters (HW) from Table I; optical-model parametrizations from OM I (Ref. 38), II (Refs. 36, 37), III (Ref. 46), IV (Ref. 47), A-3 (Ref. 48) (see the Appendix).

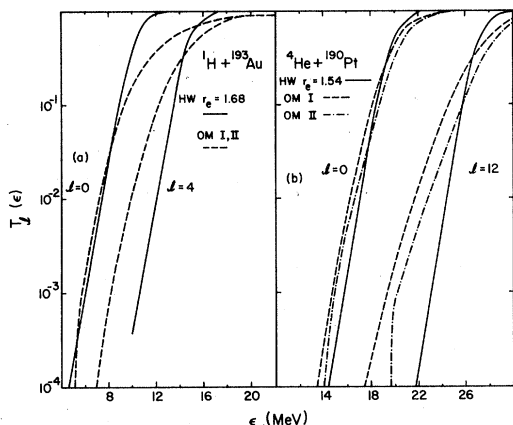


FIG. 7. Same as for Fig. 6.

has emphasized that lower transparencies are expected for excited emitting nuclei compared to ground-state nuclei due to a reduction of Pauli exclusion effects.¹⁷ (iii) The s -wave barriers differ in an unpredictable way for the HW and OM II parameter sets. As the low l waves are very important for evaporation at low energies, particular attention is needed here. We feel that elastic scattering data are especially weak for probing the small transmission coefficients for low l waves^{3,19} and are correspondingly weak for their parametrization.

Now let us turn to the role of the transmission coefficients in evaporation calculations. For a test case we choose the compound nucleus ^{194}Hg excited to 98 MeV (Ref. 14) for which many calculations have been made.^{38,39} Several results of these calculations are as follows: (i) For this system most emissions of ^4He and ^1H occur in the first decay step. (ii) Rather large variations in the level-density parameters cause little or no change in the calculated shapes of the evaporation spectra at energies below the peak energy. (The level-density parameters do, of course, affect the spectral shape at high energies.) (iii) Very small changes in the relative level-density parameters or pairing energies for the daughter nuclei can alter significantly the integrated cross section for ^1H or ^4He emission, without appreciable change in the spectral shape. (iv) The shapes of the evaporation spectra for ^4He or ^1H at low energies (below the peak) are almost exclusively dependent on the set of transmission coefficients used.

With these points in mind let us compare in Fig. 8 the calculated spectra for ^4He and ^1H from $^{194}\text{Hg}^*$. Recall that the absolute magnitudes of either calculated curve can be changed by the relative level densities. We simply want to compare the shapes of the curves at energies below the peak. For both ^1H and ^4He the curves obtained

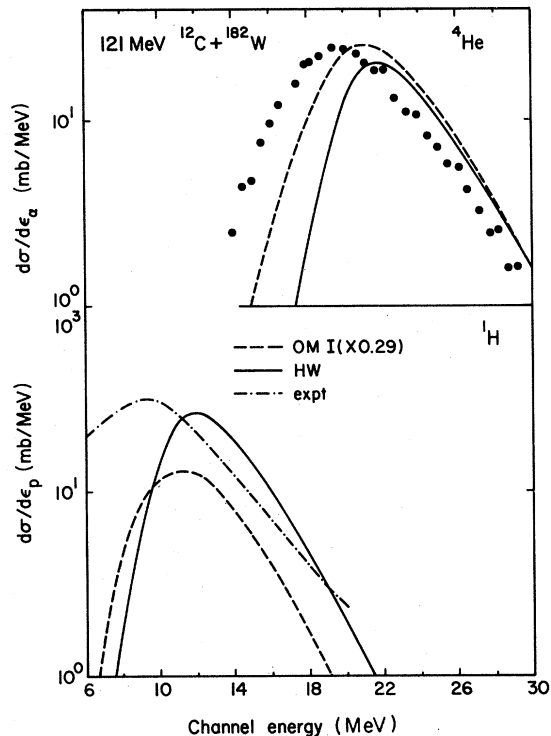


FIG. 8. Calculated evaporation spectra, from Ref. 39, for ^4He and ^1H from ^{194}Hg ($E^* = 98$ MeV, $l_{\text{crit}} = 46$). Each calculated curve is arbitrarily normalized. Hill-Wheeler parameters from Table I —; optical-model parametrization used in Ref. 38 - - -; experimental data for ^4He ●●●; - - - - for ^1H .

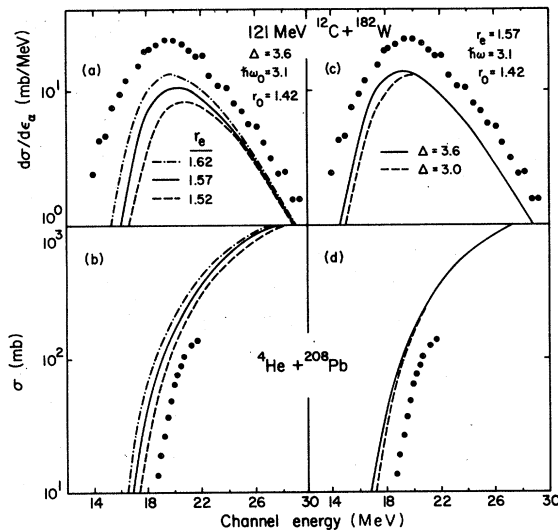


FIG. 9. (a) and (c) ^4He evaporation spectra calculated with the parameters indicated. (b) and (d) Reaction cross sections calculated with the same parameters. Experimental data are from Refs. 3 and 14.

from T_1 values from OM I (Ref. 38) are shifted to lower energies than those from HW parameters in this work. The corresponding transmission coefficients are shown in Fig. 7 along with those from OM II.^{36,37} For ${}^4\text{He}$ the $T_1(\epsilon)$ curves for both OM I and II are less steep than the HW curve. Presumably this is due to the radial extent of the absorptive potential used.²⁰ The HW set has been specifically fit to the cross section data in Fig. 4 and is therefore superior to OM II in this regard.

Even more interesting is the fact that the measured ${}^4\text{He}$ evaporation spectrum in Fig. 8 (Ref. 14) is significantly richer in low energy particles than that from either calculation. We conclude that the effective Coulomb barriers for ${}^{194}\text{Hg}^*$ ($E^* = 98$ MeV, $l_{\text{crit}} = 45$) are significantly lower than those for the ground-state species. In Fig. 9 we reverse the argument and alter the Coulomb barriers for ${}^{194}\text{Hg}^*$ in order to approach agreement with the measured evaporation spectrum. This barrier reduction can be achieved either by direct lowering of the mean barrier height (an increase in r_0) or by broadening the spectrum of barriers (an increase in Δ). Regardless of the combination of such changes, the net effect is that a barrier reduction of about 2 MeV or $\approx 10\%$ is required with respect to the reference set of T_1 values. This is clearly shown by the comparisons to fusion cross sections for ${}^4\text{He} + {}^{208}\text{Pb}$ in Figs. 9(b) and 9(d). It is interesting to compare these spectral shapes to those measured in reactions induced by 100 MeV electrons.⁴⁰ The trend of peak energies from Ref. 40 would give a peak of ≈ 22 MeV for ${}^4\text{He}$ from Hg; this value is very close to that of the calculated curve in Fig. 8 for the reference set of T_1 values we propose. The emission of ${}^4\text{He}$ has also been studied in reactions of ${}^4\text{He}$ with Ta, Au, and Pb.¹⁰ Extrapolation of these data to an Hg compound system at initial excitation of 98 MeV gives a peak energy of 20.6 ± 0.3 MeV. This value is just between those reported from ${}^{12}\text{C}$ and electron induced reactions.^{14,40} This trend seems to point toward spin of the emitting system as the cause for barrier reduction. Some additional indirect evidence for subbarrier ${}^4\text{He}$ emission has recently been presented in the reactions S+Mg, Al, (Ref. 41) and S+Ge.⁴² Some of the early work also reported surprising amounts of subbarrier H/He emission.^{9,11} However, the evaporation calculations then had many simplifications and it was not clear that they provided an adequate reference for comparison.

The liquid-drop model²⁵ does predict increasing nuclear deformations with increasing spin of the emitting nucleus. It also predicts increasing fissionability with increasing spin which would deplete the high-spin population available for ${}^4\text{He}$

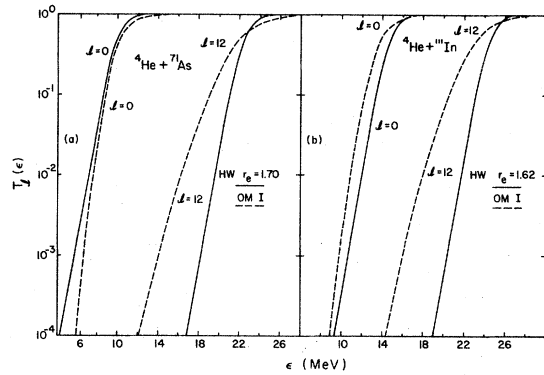


FIG. 10. Same as for Fig. 6.

evaporation.^{38,39,43,44} We defer more discussion to a more complete analysis of the nuclear evaporation.

In Figs. 10 and 11 we show T_1 curves for several other systems that have already been used in nuclear evaporation calculations. The compound nucleus ${}^{75}\text{Br}$ has been studied experimentally by Reedy *et al.*⁷ and calculations have been made by Gilat and Grover⁴⁵ and by Lu.⁴⁶ Lu has used transmission coefficients designated as OM III.⁴⁶ These curves are steeper than our reference set for $l=0$ but less steep for higher l . The net difference for calculated spectra is not easily predicted without quantitative calculations. The compound nucleus ${}^{117}\text{Te}$ has been studied by Galin *et al.*^{12,47} The

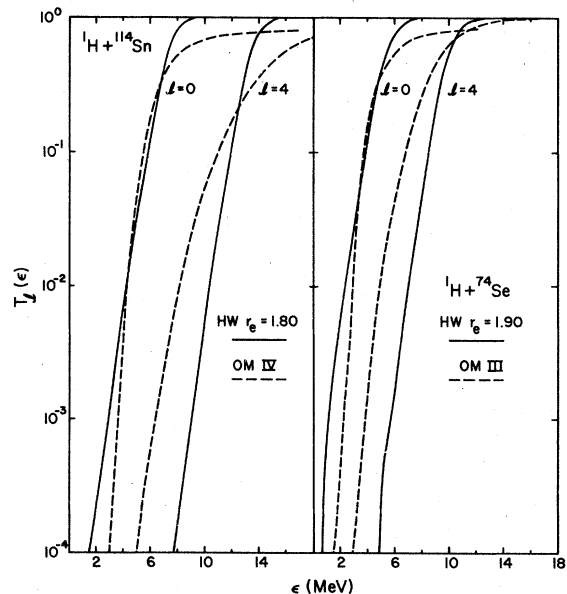


FIG. 11. Same as for Fig. 6.

transmission coefficients they used are labeled OM IV.⁴⁷ For ${}^4\text{He} + {}^{111}\text{In}$ it is clear that the HW parameter set has significantly larger effective barriers [$T_l(\epsilon)$ curves shifted to higher energies] than the OM IV set used in the Galin analysis.⁴⁷ It follows that this HW reference set of T_l values will give many fewer low energy evaporated ${}^4\text{He}$ particles than given by the Galin calculations.⁴⁷ As the Galin analysis did fit the experimental data we would expect a misfit for the HW set, similar to that shown in Figs. 8 and 9 for ${}^{194}\text{Hg}$. This expectation should nevertheless be tested by direct calculations.

IV. SUMMARY

It is reemphasized that fusion reactions are the inverse of evaporative decay.¹⁵⁻¹⁷ Hence, the view is taken that transmission coefficients for evaporation calculations are more appropriately related to fusion cross sections than to elastic scattering. From the available experimental data for fusion we obtain a systematic set of effective barrier parameters for ${}^1\text{H}$ and ${}^4\text{He}$ reactions. We propose this parameter set only as a source of reference values of transmission coefficients. Comparisons of measured evaporation spectra to those calculated with these reference values of T_l can give insight into the changes in effective barriers between ground-state nuclei and excited nuclei.¹⁷ Such a comparison for ${}^{194}\text{Hg}$ ($E^* = 98$ MeV, $l_{\text{crit}} = 45$) implies a significant barrier reduction for this excited nucleus.

ACKNOWLEDGMENTS

We appreciate the comments of H. Delagrange and his help with the program GROGIF and the A-3 calculations. The authors of Ref. 14 have allowed us to use their data in Fig. 8, prior to publication. M. Beckerman and M. Blann have been very helpful with their program MB-II.

APPENDIX

Following the procedure of Refs. 20 and 22, Delagrange, Vaz, and Alexander⁴⁸ have modified the proximity potential to fit fusion and elastic scattering cross sections for several systems including ${}^4\text{He} + {}^{208}\text{Pb}$. They have used the optical-model code A-THREE of Auerbach.⁴⁹ The empirical s -wave barrier they obtain is ≈ 0.25 MeV lower than that obtained from the fit by Eq. (6). For $E_{\text{c.m.}} > 17$ MeV their fit is only slightly better than

that from Eq. (6), but for $\sigma_{\text{cf}} \lesssim 1$ mb or $E_{\text{c.m.}} \lesssim 17$ MeV their calculated excitation function for fusion becomes noticeably steeper. This is due to the significantly greater thickness of the nuclear plus Coulomb potential compared to the parabolic simulation. In addition, and for the same reason, the shapes of the $T_l(\epsilon)$ curves from this model are slightly steeper than those from Eq. (7) (shown in Fig. 6).

What would be the result of these differences for evaporation calculations as shown, for example, in Figs. 8 and 9? For evaporation essentially unconstrained by angular momentum [as for this case of ${}^{194}\text{Hg}$ (Refs. 38 and 39)], only the inverse cross section for all partial waves is important. For ${}^4\text{He} + {}^{208}\text{Pb}$ we have said that the fits to σ_{cf} are equivalent for $E \geq 17$ MeV. For ${}^{194}\text{Hg}$ presumably this equivalency would hold to $(78/82)$ 17 MeV or to ≈ 16 MeV. In Fig. 8 we see that at ≈ 16 MeV the calculated ${}^4\text{He}$ evaporation spectrum would be reduced to < 0.01 of the peak value. Hence, for this case the difference should be negligible.

What would be the effect on the calculated l distribution for the evaporated ${}^4\text{He}$? The more realistic potential is more difficult to penetrate than is the parabola, and therefore gives steeper curves for $T_l(\epsilon)$. (Compared to the parabolic simulation these curves cross for $l=0$ at $T_{l=0} \approx 0.03$ and for $l=10$ at $T_{l=10} \approx 0.006$.) Hence, the l distribution for evaporated ${}^4\text{He}$ will be driven closer to the sharp-cutoff distribution. This is exactly the opposite to the curves shown in Fig. 7 for OM I and II compared to the HW curve from Eq. (7). Presumably this is due to a stronger imaginary potential in the surface for OM I and II. This is a very common result for two and four parameter optical-model fits to elastic scattering alone. The thrust of this paper is that the most reasonable calibration of the inverse cross sections is that which is derived from fusion cross sections. Furthermore, even the simple Hill-Wheeler formula [Eq. (7)] can give empirical fits to these fusion excitation functions over the energy region of most interest for evaporation calculations. More realistic potentials, if properly parametrized, may provide a more satisfactory l distribution for the evaporated particles which could be important near the yrast line. However, it may well be that most high-spin compound nuclei are so heavily deformed that the estimation of these shape changes is more important than refinement of the form of the angle-independent potential for ground-state nuclei. Figures 7-11 make this point more clear.

- ¹J. M. D'Auria, M. J. Fluss, L. Kowalski, and J. M. Miller, *Phys. Rev.* **168**, 1224 (1968).
- ²R. Broda, M. Ishihara, B. Herskind, H. Oeschler, and S. Ogaza, *Nucl. Phys.* **A248**, 356 (1975).
- ³A. R. Barnett and J. S. Lilley, *Phys. Rev. C* **9**, 2010 (1974).
- ⁴W. J. Ramler, J. Wing, D. J. Henderson, and J. R. Huizenga, *Phys. Rev.* **114**, 154 (1959).
- ⁵H. Freiesleben and J. R. Huizenga, *Nucl. Phys.* **A224**, 503 (1974).
- ⁶S. Y. Lin and J. M. Alexander, *Phys. Rev. C* **16**, 688 (1977).
- ⁷J. Wing and J. R. Huizenga, *Phys. Rev.* **128**, 280 (1962).
- ⁸J. R. Boyce, T. D. Hayward, R. Bass, H. W. Newson, E. G. Bilpuch, F. O. Purser, and H. W. Schmitt, *Phys. Rev. C* **10**, 231 (1974); J. R. Boyce, Ph.D. thesis, Duke University, 1972.
- ⁹Some examples of the early work are as follows: W. J. Knox, A. R. Quinton, and C. E. Anderson, *Phys. Rev.* **120**, 2120 (1960); F. E. Durham and M. L. Halbert, *ibid.* **137**, B850 (1965); H. C. Britt and A. R. Quinton, *ibid.* **124**, 877 (1961); C. Brun, B. Gatty, M. Lefort, and X. Tarrago, *Nucl. Phys.* **A116**, 177 (1968); J. Benveniste, G. Merkel, and A. Mitchell, *Phys. Rev.* **174**, 1357 (1968).
- ¹⁰G. Chenevert, I. Halpern, B. G. Harvey, and D. L. Hendrie, *Nucl. Phys.* **A122**, 481 (1968).
- ¹¹R. C. Reedy, M. J. Fluss, G. F. Herzog, L. Kowalski, and J. M. Miller, *Phys. Rev.* **188**, 1771 (1969); J. M. D'Auria, M. J. Fluss, G. Herzog, L. Kowalski, J. M. Miller, and R. C. Reedy, *ibid.* **174**, 1409 (1968).
- ¹²J. Galin, B. Gatty, D. Guerreau, C. Rousset, V. C. Schlothauer-Voos, and X. Tarrago, *Phys. Rev. C* **9**, 1113 (1974); **9**, 1126 (1974).
- ¹³T. Nomura, H. Utsunomiya, T. Motabayashi, T. Inamura, and M. Yanokura, *Phys. Rev. Lett.* **40**, 694 (1978).
- ¹⁴J. M. Miller, D. Logan, G. L. Catchen, M. Rajagopalan, J. M. Alexander, M. Kaplan, J. W. Ball, M. S. Zisman, and L. Kowalski, *Phys. Rev. Lett.* **40**, 1074 (1978).
- ¹⁵H. A. Bethe, *Rev. Mod. Phys.* **9**, 71 (1937).
- ¹⁶J. M. Blatt and V. F. Weisskopf, *Theoretical Nuclear Physics* (Wiley, New York, 1952).
- ¹⁷T. Ericson, *Adv. Phys.* **9**, 425 (1960).
- ¹⁸L. W. Put and A. M. J. Paans, *Nucl. Phys.* **A291**, 93 (1977).
- ¹⁹I. Badawy, B. Berthier, P. Charles, M. Dost, B. Fernandez, J. Gastebois, and S. M. Lee, *Phys. Rev. C* **17**, 978 (1978).
- ²⁰L. C. Vaz, J. M. Alexander, and E. H. Auerbach, *Phys. Rev. C* **18**, 820 (1978).
- ²¹L. C. Vaz and J. M. Alexander, *Phys. Rev. C* **18**, 833 (1978).
- ²²L. C. Vaz and J. M. Alexander, *Phys. Rev. C* **18**, 2152 (1978).
- ²³J. B. Ball, C. B. Fulmer, E. E. Grass, M. L. Halbert, D. C. Hensley, C. A. Ludemann, M. J. Saltmarsh, and G. R. Satchler, *Nucl. Phys.* **A252**, 208 (1975).
- ²⁴F. Videbaek, R. B. Goldstein, L. Grodzins, S. G. Steadman, T. A. Belote, and J. G. Garrett, *Phys. Rev. C* **15**, 954 (1977).
- ²⁵S. Cohen, F. Plasil, and W. J. Swiatecki, *Ann. Phys. (N.Y.)* **82**, 557 (1974).
- ²⁶G. Sauer, H. Chandra, and U. Mosel, *Nucl. Phys.* **A264**, 221 (1976).
- ²⁷M. Beckerman and M. Blann (unpublished).
- ²⁸M. Lefort, *J. Phys. (Paris)* **C5**, 57 (1976); M. Blann, in *Proceedings of the International Conference on Nuclear Physics, Munich, 1973*, edited by J. de Boer and H. J. Mang (North-Holland, Amsterdam/American Elsevier, New York, 1973), Vol. II, p. 667.
- ²⁹E. K. Hyde, I. Perlman, and G. T. Seaborg, *Nuclear Properties of the Heavy Elements* (Prentice-Hall, Englewood Cliffs, New Jersey, 1964).
- ³⁰L. C. Vaz and J. M. Alexander, *Phys. Rev. C* **10**, 464 (1974), and references therein.
- ³¹C. Y. Wong, *Phys. Lett.* **42B**, 186 (1972); *Phys. Rev. Lett.* **31**, 766 (1973).
- ³²T. Kodama, R. A. M. S. Nazareth, P. Moller, and J. R. Nix, *Phys. Rev. C* **17**, 111 (1978).
- ³³D. L. Hill and J. A. Wheeler, *Phys. Rev.* **89**, 1102 (1953).
- ³⁴J. Blocki, J. Randrup, W. J. Swiatecki, and C. F. Tsang, *Ann. Phys. (N.Y.)* **105**, 427 (1977).
- ³⁵J. M. Alexander, L. C. Vaz, and S. Y. Lin, *Phys. Rev. Lett.* **25**, 1487 (1974).
- ³⁶D. Wilmore and P. E. Hodgson, *Nucl. Phys.* **55**, 673 (1964); F. G. Perey and B. Buck, *ibid.* **32**, 353 (1962); F. G. Perey, *Phys. Rev.* **131**, 745 (1963); G. R. Satchler, *Nucl. Phys.* **70**, 177 (1965).
- ³⁷The "bumpy" shapes for low T_i values are from cutoffs in the particular code used; they could be easily corrected and have no real significance in comparing the parametrizations. They could, of course, be serious for some evaporation calculations. M. Beckerman and M. Blann, University of Rochester, Nuclear Structure Research Laboratory Report No. UR-NSRL-135, MB-II description.
- ³⁸H. Delagrange, A. Fleury, and J. M. Alexander, *Phys. Rev. C* **16**, 706 (1977); T_i values from G. S. Mani, M. A. Melkanoff, and I. Iori, CEA Reports Nos. 2379 and 2380, 1963 (unpublished); J. R. Huizenga and G. I. Igo, Argonne National Laboratory Report No. 6373, 1961 (unpublished).
- ³⁹M. A. McMahan, Ph.D. thesis, Department of Chemistry, Columbia University, New York, N. Y. 10027 (in preparation).
- ⁴⁰J. J. Murphy II, H. J. Gehrhardt, and D. M. Skopik, *Nucl. Phys.* **A277**, 69 (1977).
- ⁴¹F. Puhlhofer, W. F. W. Schneider, F. Busch, J. Barrette, P. Braun-Munzinger, C. K. Gelpke, and H. E. Wagner, *Phys. Rev. C* **16**, 1010 (1977).
- ⁴²D. Horn, H. A. Enge, A. Sperduto, and A. Graue, *Phys. Rev. C* **17**, 118 (1978).
- ⁴³M. Beckerman and M. Blann, *Phys. Rev. Lett.* **38**, 272 (1977); *Phys. Lett.* **68B**, 31 (1977).
- ⁴⁴M. Blann and F. Plasil, *Phys. Rev. Lett.* **29**, 303 (1972).
- ⁴⁵J. Gilat and J. R. Grover, *Phys. Rev. C* **3**, 734 (1971); T_i values from F. Bjorklund and S. Fernbach, *ibid.* **109**, 1295 (1958); F. G. Perey, *ibid.* **131**, 745 (1963); J. R. Huizenga and G. Igo, *Nucl. Phys.* **29**, 462 (1962).
- ⁴⁶N. H. Lu, private communication (1977); T_i values from A. Budzanowski, A. Dudek, K. Grotowski, J.

Kuzninski, N. Niewodniczanski, A. Strzalkowki, J. Szmidox, and R. Wolski, Institute of Nuclear Physics, Krakow, Poland, Report No. INP-441/P, 1965 (unpublished); F. G. Perey, Phys. Rev. 131, 745 (1963).

⁴⁷J. Galin, B. Gatty, D. Guerreau, V. C. Schlotthauer-Voos, and X. Tarrago, Phys. Rev. C 10, 638 (1974);

T_i values from F. Bjorklund and S. Fernbach, *ibid.* 109, 1295 (1958); J. R. Huizenga and G. Igo, Nucl. Phys. 29, 462 (1962).

⁴⁸H. Delagrange, L. C. Vaz, and J. M. Alexander, Phys. Rev. C, to be published.

⁴⁹E. H. Auerbach, Comput. Phys. Commun. 15, 165 (1978).